Available online at www.sciencedirect.com
ScienceDirect
IFAC PapersOnLine 56-2 (2023) 6789–6795

Implicit port-Hamiltonian systems: structure-preserving discretization for the nonlocal vibrations in a viscoelastic nanorod, and for a seepage model ⋆

Antoine Bendimerad-Hohl * **Ghislain Haine** *
Laurent Lefèvre ** **Denis Matignon** *

* *Institut Supérieur de l'Aéronautique et de l'Espace (ISAE-Supaero), Université de Toulouse, 10 Avenue Edouard Belin, 31055 Toulouse Cedex 4, France*
** *Univ. Grenoble Alpes, Grenoble INP*†*, LCIS, Valence, France*
† *Institute of Engineering Univ. Grenoble Alpes*
antoine.bendimerad-hohl@student.isae-supaero.fr ghislain.haine@isae.fr
laurent.lefevre@lcis.grenoble-inp.fr denis.matignon@isae.fr

Abstract: A structure-preserving partitioned finite element method (PFEM), for the semi-discretization of infinite-dimensional explicit port-Hamiltonian systems (pHs), is extended to those pHs of implicit type, leading to port-Hamiltonian Differential Algebraic Equations (pH-DAE). Two examples are dealt with: the nonlocal vibrations in a viscoelastic nanorod in 1D, and the dynamics of a fluid filtration model, the Dzektser seepage model in 2D, for which illustrative numerical simulations are provided.

Copyright © 2023 The Authors. This is an open access article under the CC BY-NC-ND license (https://creativecommons.org/licenses/by-nc-nd/4.0/)

Keywords: port-Hamiltonian systems, Structure-Preserving Discretization, Partitioned Finite Element Method, Implicit port-Hamiltonian systems, Nonlocal dynamics.

1. INTRODUCTION

The port-Hamiltonian systems (pHs) formalism has proven to be a powerful tool for the modelling and control of complex multiphysics systems (van der Schaft et al. (2014); Duindam et al. (2009)). This framework has been extended to the case of distributed parameter systems, i.e. when spatio-temporal dynamics are taken into account, see e.g. van der Schaft and Maschke (2002); Jacob and Zwart (2012); Rashad et al. (2020). Besides 1D examples, 2D and 3D problems have also been recently considered, either from a mathematical point of view (Kurula and Zwart, 2015), or modelling, simulation or control perspectives (Vu et al. (2016); Altmann and Schulze (2017); Brugnoli et al. (2019); Cardoso-Ribeiro et al. (2019); Bendimerad-Hohl et al. (2022)). In particular, structure-preserving spatial discretization methods have been proposed which lead to finite-dimensional continuous-time port-Hamiltonian systems approximations for such 2D or 3D models with non autonomous boundary conditions (Kotyczka et al. (2018); Cardoso-Ribeiro et al. (2021); Brugnoli et al. (2021)), together with convergence results in the sense of numerical analysis (Haine et al., 2023).

Even more recently, distributed parameter models given in implicit form (implicit partial differential equations), either singular or not, have been considered in this pHs settings (see for instance Yaghi et al. (2022) for a pHs formulation of the Allen-Cahn model governing some solidification process dynamics, Jacob and Morris (2022) for investigation on a pHs model of the Dzektser equation (Dzektser (1972)) modelling the seepage of underground water or Heidari and Zwart (2019) for the pHs formulation of non-local elastic vibrations (Eringen (1983)) in a nanorod. On the other hand, finite-dimensional Port-Hamiltonian Differential-Algebraic systems (pH-DAEs) have been intensively studied (see for instance Beattie et al. (2018) for linear descriptor systems in matrix representation, Mehrmann and Unger (2022) for control applications of such systems, Mehrmann and Morandin (2019) for structure-preserving discretization or more recently van der Schaft and Maschke (2018, 2020); Mehrmann and van der Schaft (2023) for geometric representations both in the linear and nonlinear cases.

In this paper we focus on the problem of structure-preserving spatial discretization of implicit infinite-dimensional pHs. In particular we show how the Partitioned Finite Element Method (PFEM, see Cardoso-Ribeiro et al. (2021)) carries over to the implicit case and gives rise to a set of pH-DAEs. The proposed method is applied on two examples related respectively to non-local viscoelastic constitutive equations and to ground waters motion with free surface. Numerical simulations are presented to illustrate the properties of the proposed method.

⋆ This work was partially supported by the AID from the French Ministry of the Armed Forces, and by the IMPACTS project, entitled *IMplicit Port-HAmiltonian ConTrol Systems*, funded by the French National Research Agency (ANR) [Grant Agreement No. ANR-21-CE48-0018]. Further information is available at https://impacts.ens2m.fr/.

2405-8963 Copyright © 2023 The Authors. This is an open access article under the CC BY-NC-ND license.
Peer review under responsibility of International Federation of Automatic Control.
10.1016/j.ifacol.2023.10.387

The paper is organized as follows: in § 2 the non-local longitudinal vibrations in a viscoelastic nanorod presented in Heidari and Zwart (2019) are recalled, making use of the theory of nonlocal elasticity; the application of the Partitioned Finite Element Method (PFEM) to this pHs of implicit type is presented in details, and leads to a pH-DAE with the natural choice of a Hamiltonian functional. In § 3, another implicit system is presented and corrected from the literature: the Dzektser PDE, describing a seepage model. A Hamiltonian formulation is derived first, and PFEM is applied to it, leading to a pH-DAE. This second model is different from the first one, in so far as the implicit nature comes from an unbounded differential operator, namely $\mathrm{Id} - \varepsilon^2\Delta$, and no more from a singular square matrix E. Moreover, in § 3.4, simulations results are provided, showing the influence of the non-local parameter ε.

2. NONLOCAL LONGITUDINAL VIBRATIONS IN A VISCOELASTIC NANOROD

In § 2.1, the formulation of the dynamics is presented with a first choice of Hamiltonian functional which leads to a descriptor system, or implicit pHs with a singular matrix; then in § 2.2, the Partitioned Finite Element Method is applied to this system, which leads to a pH-DAE.

2.1 First Hamiltonian formulation

Let us define $\Omega = [0, \ell]$ the spatial domain, $w(x,t)$ the longitudinal displacement, $N(x,t)$ the longitudinal force applied to the nanorod, ρ the linear mass density and A the cross section area.

Following Heidari and Zwart (2019), a Hamiltonian for the nanorod vibration system is given by

$$\mathcal{H} := \frac{1}{2}\int_\Omega \left(a^2 w^2 + \rho A \left(\frac{\partial w}{\partial t}\right)^2 + \mu\rho A \left(\frac{\partial^2 w}{\partial t \partial x}\right)^2 + (EA + \mu a^2)\left(\frac{\partial w}{\partial x}\right)^2 \right),$$

where a is the stiffness coefficient of the viscoelastic layer, μ the non local parameter and E elastic modulus of the nanorod. Let us choose the state variables as $z := \left(w,\ \rho A\frac{\partial w}{\partial t},\ \mu\rho A\frac{\partial^2 w}{\partial t\partial x},\ \frac{\partial w}{\partial x},\ N\right)^\top$. ω is the displacement, $\rho A\frac{\partial w}{\partial t}$ the momentum density, $\mu\rho A\frac{\partial^2 w}{\partial t\partial x}$ the flow variable of the non locality, $\frac{\partial w}{\partial x}$ the strain and N the stress resultant.

Denoting

$$\mathbb{E} := \begin{pmatrix} 1&0&0&0&0\\ 0&1&0&0&0\\ 0&0&1&0&0\\ 0&0&0&1&0\\ 0&0&0&0&0 \end{pmatrix}, \qquad Q := \begin{pmatrix} a^2 & 0 & 0 & 0 & 0\\ 0 & \frac{1}{\rho A} & 0 & 0 & 0\\ 0 & 0 & \frac{1}{\mu\rho A} & 0 & 0\\ 0 & 0 & 0 & EA+\mu a^2 & 0\\ 0&0&0&0&1 \end{pmatrix},$$

the Hamiltonian $\mathcal{H}$ rewrites $\mathcal{H} = \frac{1}{2}\int_\Omega z^\top \mathbb{E}^\top Q z$, with the important algebraic property $\mathbb{E}^\top Q = Q^\top \mathbb{E}$.

Defining furthermore

$$J := \begin{pmatrix} 0 & 1 & 0 & 0 & 0\\ -1 & 0 & 0 & 0 & \frac{\partial}{\partial x}\\ 0 & 0 & 0 & -1 & 1\\ 0 & 0 & 1 & 0 & 0\\ 0 & \frac{\partial}{\partial x} & -1 & 0 & 0 \end{pmatrix}, \quad R := \begin{pmatrix} 0 & 0 & 0 & 0 & 0\\ 0 & b^2 & 0 & 0 & 0\\ 0 & 0 & \tau_d EA + \mu b^2 & 0 & 0\\ 0&0&0&0&0\\ 0&0&0&0&0 \end{pmatrix},$$

where b is the damping coefficient of the viscoelastic layer and τ_d the viscous damping of the nanorod.

The dynamics of the system is given by

$$\mathbb{E}\dot{z}(t) = (J - R)e(t), \qquad e = Qz. \tag{1}$$

Finally, the power balance reads (Heidari and Zwart, 2019, eq. (20))

$$\frac{\mathrm{d}}{\mathrm{d}t}\mathcal{H} = \frac{1}{2}\left[\frac{\partial w}{\partial t}N\right]_0^\ell - \int_\Omega \left(b^2\left(\frac{\partial w}{\partial t}\right)^2 + (\tau_d EA + \mu b^2)\left(\frac{\partial^2 w}{\partial t\partial x}\right)^2 \right),$$

or more compactly

$$\frac{\mathrm{d}}{\mathrm{d}t}\mathcal{H}(t) = -\int_\Omega e(t,x)\cdot Re(t,x)\mathrm{d}x + [u(t,s)y(t,s)]_0^\ell, \tag{2}$$

where u and y stand for boundary control and boundary observation. More precisely, let us recall $e_2 = \frac{\partial w}{\partial t}$ and $e_5 = N$. Therefore the boundary product of the control and the observation must result in the product between the *velocity* and the *force* at the boundary: $u = N, y = \frac{\partial w}{\partial t}$.

2.2 The Partitioned Finite Element Method

Variational formulation Let us consider test functions $\lambda_1, \ldots, \lambda_5 \in D(\Omega)$ on the domain.

The variational formulation of (1) is given by

$$\begin{cases} \int_\Omega \lambda_1 \dot{z}_1 = \int_\Omega \lambda_1 e_2,\\ \int_\Omega \lambda_2 \dot{z}_2 = -\int_\Omega \lambda_2(e_1 + \lambda_2 b^2 e_2) + \int_\Omega \lambda_2 \frac{\partial e_5}{\partial x},\\ \int_\Omega \lambda_3 \dot{z}_3 = \int_\Omega \lambda_3(-e_4 + e_5) - \int_\Omega \lambda_3(\tau_d EA + \mu b^2)e_3,\\ \int_\Omega \lambda_4 \dot{z}_4 = \int_\Omega \lambda_4 e_3,\\ 0 = \int_\Omega \lambda_5 \frac{\partial e_2}{\partial x} - \int_\Omega \lambda_5 e_3, \end{cases} \tag{3}$$

together with the constitutive relations

$$\begin{cases} \int_\Omega \lambda_1 e_1 = \int_\Omega a^2 \lambda_1 z_1,\\ \int_\Omega \lambda_2 e_2 = \int_\Omega \frac{1}{\rho A}\lambda_2 z_2,\\ \int_\Omega \lambda_3 e_3 = \int_\Omega \frac{1}{\mu\rho A}\lambda_3 z_3,\\ \int_\Omega \lambda_4 e_4 = \int_\Omega (EA + \mu a^2)\lambda_4 z_4,\\ \int_\Omega \lambda_5 e_5 = \int_\Omega \lambda_5 z_5. \end{cases} \tag{4}$$

Choice of causality The next step is to choose a causality. By using an integration by parts on the differential term of the second or fifth line of (3), the control term will appear.

Let us choose the control u as the (normal trace of the) *force*. To do so, we will integrate by part on the *second* line of (3)

$$\int_\Omega \lambda_2 \frac{\partial e_5}{\partial x} = -\int_\Omega \frac{\partial \lambda_2}{\partial x} e_5 + [\,\lambda_2 e_5\,]_0^\ell.$$

Here $e_5 = N$ appears as the boundary term.

Finite elements families Let us choose 5 families $(\lambda_{1,i})_{i\in[\![1,n_1]\!]}$, $(\lambda_{2,i})_{i\in[\![1,n_2]\!]}$, $\ldots$, $(\lambda_{5,i})_{i\in[\![1,n_5]\!]}$ of finite elements in $H^1(\Omega)$ of size $n_1,\ldots,n_5 \in \mathbb{N}$ respectively. And $\psi_1 = \delta_0, \psi_2 = \delta_l$ the finite element family of the control at the boundary $\{0,\ell\}$.

Let us denote the approximations of z_i, e_i, u and y as

$$\begin{cases} z_i^d := \sum_{j=1}^{n_i} \lambda_{i,j}(x)\underline{z}_{i,j}(t), & \forall i \in [\![1,5]\!], \\ e_i^d := \sum_{j=1}^{n_i} \lambda_{i,j}(x)\underline{e}_{i,j}(t), & \forall i \in [\![1,5]\!], \\ u^d := \sum_{j=1}^{2} \psi_j(x)\underline{u}_j(t), \qquad y^d := \sum_{j=1}^{2} \psi_j(x)\underline{y}_j(t). \end{cases}$$

Substituting these approximations in the variational formulation (3) leads to

$$\mathbf{E}\dot{\underline{z}}(t) = (\mathbf{J} - \mathbf{R})\,\underline{e}(t) + \mathbf{B}\underline{u}(t), \tag{5}$$

where $\underline{z} := \left(\underline{z}_{1,1},\ldots,\underline{z}_{1,n_1},\underline{z}_{2,1},\ldots,\underline{z}_{2,n_2},\underline{z}_{3,1},\ldots,\underline{z}_{5,n_5}\right)^\top$ and similarly for $\underline{e}$, $\underline{u} := (\underline{u}_1,\underline{u}_2)^\top$,$\underline{y} := \left(\underline{y}_1,\underline{y}_2\right)^\top$, and

$$\mathbf{E} := \begin{pmatrix} \mathbf{M}^{1,1} & 0 & 0 & 0 & 0 \\ 0 & \mathbf{M}^{2,2} & 0 & 0 & 0 \\ 0 & 0 & \mathbf{M}^{3,3} & 0 & 0 \\ 0 & 0 & 0 & \mathbf{M}^{4,4} & 0 \\ 0 & 0 & 0 & 0 & 0 \end{pmatrix},$$

$$\mathbf{J} := \begin{pmatrix} 0 & \mathbf{M}^{1,2} & 0 & 0 & 0 \\ -\mathbf{M}^{1,2^T} & 0 & 0 & 0 & -\mathbf{D} \\ 0 & 0 & 0 & -\mathbf{M}^{3,4} & \mathbf{M}^{3,5} \\ 0 & 0 & \mathbf{M}^{3,4^T} & 0 & 0 \\ 0 & \mathbf{D}^T & -\mathbf{M}^{3,5^T} & 0 & 0 \end{pmatrix},$$

$$\mathbf{R} := \begin{pmatrix} 0 & 0 & 0 & 0 & 0 \\ 0 & b^2\mathbf{M}^{2,2} & 0 & 0 & 0 \\ 0 & 0 & (\tau_d EA + \mu b^2)\mathbf{M}^{3,3} & 0 & 0 \\ 0 & 0 & 0 & 0 & 0 \\ 0 & 0 & 0 & 0 & 0 \end{pmatrix},$$

and

$$\mathbf{B} := \begin{pmatrix} 0 & \mathbf{B}_p^\top & 0 & 0 & 0 \end{pmatrix}^\top,$$

with

$$\mathbf{M}^{i,j} := \left(\int_\Omega \lambda_{i,k}\lambda_{j,l}\right)_{k\in[\![1,n_i]\!],l\in[\![1,n_j]\!]} \in \mathbb{R}^{n_i\times n_j},$$

$$\mathbf{D} := \left(\int_\Omega \frac{\partial \lambda_{2,k}}{\partial x}\lambda_{5,l}\right)_{k\in[\![1,n_2]\!],l\in[\![1,n_5]\!]} \in \mathbb{R}^{n_2\times n_5},$$

and

$$\mathbf{B}_p := \left(\int_{\partial\Omega} \lambda_{2,k}\psi_l\right)_{k\in[\![1,n_2]\!],l=1,2} \in \mathbb{R}^{n_2\times 2}.$$

Similarly, substituting the approximation into the variational formulation of the constitutive relations (4) leads to

$$\mathbf{M}\underline{e}(t) = \mathbf{Q}\underline{z}(t), \tag{6}$$

where

$$\mathbf{M} := \begin{pmatrix} \mathbf{M}^{1,1} & 0 & 0 & 0 & 0 \\ 0 & \mathbf{M}^{2,2} & 0 & 0 & 0 \\ 0 & 0 & \mathbf{M}^{3,3} & 0 & 0 \\ 0 & 0 & 0 & \mathbf{M}^{4,4} & 0 \\ 0 & 0 & 0 & 0 & \mathbf{M}^{5,5} \end{pmatrix},$$

with $\mathbf{M}^{i,i}$ are symmetric square matrices, and

$$\mathbf{Q} := \begin{pmatrix} a^2\mathbf{M}^{1,1} & 0 & 0 & 0 & 0 \\ 0 & \frac{1}{\rho A}\mathbf{M}^{2,2} & 0 & 0 & 0 \\ 0 & 0 & \frac{1}{\mu\rho A}\mathbf{M}^{3,3} & 0 & 0 \\ 0 & 0 & 0 & (EA+\mu a^2)\mathbf{M}^{4,4} & 0 \\ 0 & 0 & 0 & 0 & \mathbf{M}^{5,5} \end{pmatrix}$$

Finally, the discretized observation reads

$$\underline{y}(t) = \mathbf{B}^\top \underline{e}(t), \tag{7}$$

Gathering (5)–(6)–(7) gives the discrete port-Hamiltonian system

$$\begin{cases} \mathbf{E}\dot{\underline{z}}(t) = (\mathbf{J} - \mathbf{R})\,\underline{e}(t) + \mathbf{B}\underline{u}(t), \\ \mathbf{M}\underline{e}(t) = \mathbf{Q}\underline{z}(t), \\ \underline{y}(t) = \mathbf{B}^\top \underline{e}(t). \end{cases}$$

Let us now consider the discrete Hamiltonian defined as

$$\mathcal{H}^d(t) := \frac{1}{2}\int_\Omega z^d(t)^\top \mathbb{E}^\top e^d(t) = \frac{1}{2}\underline{z}(t)^\top \mathbf{E}^\top \underline{e}(t). \tag{8}$$

The algebraic property $\mathbb{E}^\top Q = Q^\top \mathbb{E}$ translates into $\mathbf{E}^\top\mathbf{M}^{-1}\mathbf{Q} = \mathbf{Q}\mathbf{M}^{-1}\mathbf{E}$, which is satisfied with the previous definitions of the matrices $\mathbf{E}$, $\mathbf{M}$ and $\mathbf{Q}$.

With this property at hand, one gets for the discrete balance equation, using (6)

$$\begin{aligned} \frac{\mathrm{d}}{\mathrm{d}t}\mathcal{H}^d(t) &= \frac{1}{2}\dot{\underline{z}}(t)^\top \mathbf{E}^\top \underline{e}(t) + \frac{1}{2}\underline{z}(t)^\top \mathbf{E}^\top \dot{\underline{e}}(t) \\ &= \frac{1}{2}\dot{\underline{z}}(t)^\top \mathbf{E}^\top \underline{e}(t) + \frac{1}{2}\underline{z}(t)^\top \mathbf{E}^\top \mathbf{M}^{-1}\mathbf{Q}\dot{\underline{z}}(t) \\ &= \frac{1}{2}\dot{\underline{z}}(t)^\top \mathbf{E}^\top \underline{e}(t) + \frac{1}{2}\underline{z}(t)^\top \mathbf{Q}\mathbf{M}^{-1}\mathbf{E}\dot{\underline{z}}(t) \\ &= \frac{1}{2}\dot{\underline{z}}(t)^\top \mathbf{E}^\top \underline{e}(t) + \frac{1}{2}\underline{e}(t)^\top \mathbf{E}\dot{\underline{z}}(t) \\ &= \dot{\underline{z}}(t)^\top \mathbf{E}^\top \underline{e}(t), \end{aligned}$$

Using (5) and (7) then gives the discrete power balance

$$\frac{\mathrm{d}}{\mathrm{d}t}\mathcal{H}^d(t) = -\underline{e}(t)^\top \mathbf{R}\underline{e}(t) + \underline{u}(t)^\top \underline{y}(t),$$

which stands for the discrete counterpart of (2).

This justifies the definition (8) of the discrete Hamiltonian. The same derivation applies to the case of space-varying coefficients, which could aslo be considered.

Remark 1 In Heidari and Zwart (2019), a second Hamiltonian functional is proposed, involving G a symmetric integral operator: it gives rise to a pH-ODE.The compact operator G is making explicit the implicit part $(1 - \mu\,\frac{d^2}{dx^2})$ of the original formulation. Applying PFEM now leads to a $\mathbf{G}$ matrix which is dense, and no more sparse, as the discrete counterpart of the G operator: thus, even in the 1D case, one has to deal with an increased computational burden; the situation would be even worse in 2D.

3. DZEKTSER EQUATION

The Dzektser equation allows for modelling the seepage of underground water and is a generalization of the Boussinesq equation.

Let us define h_0 the hydraulic head, $\bar{h_0}$ the mean hydraulic head, μ the coefficient of free porosity, k the permeability of the medium, ϵ_0 and ϵ_a the quantities for feeding the flow through its base and free surface. The Dzektser equation is then written in 2D as

$$(1-\varepsilon^2\Delta)\frac{\partial h_0}{\partial t} = \frac{k}{\mu}\bar{h_0}\Delta h_0 - \frac{\bar{h_0}^3}{2\mu\beta^2}\Delta^2 h_0 + \frac{\epsilon_0+\epsilon_a}{\mu}\beta,$$

where $\varepsilon := \frac{\bar{h_0}}{\sqrt{2\beta}}$ is the *characteristic length* of the non-local effect. In the sequel we will consider $\epsilon_0 = \epsilon_a = 0$, and a control at the boundary of the 2D horizontal domain.

Remark 2 Note that the minus sign in front of the Laplacian operator is to be found in (Dzektser, 1972, eq (24)), and cited as such in e.g. Perevozhikova and Manakova (2021). However, in several related works (Fedorov and Shklyar, 2012; Ge et al., 2020; Jacob and Morris, 2022), it has been transformed into a plus sign, giving rise to a singularity, since in this case the unbounded differential operator has a nonzero kernel, a mathematical artifact which is not based on any physical ground.

3.1 Port-Hamiltonian formulation

Let us note $a = \frac{k}{\mu}\bar{h_0}, \quad b = \frac{\bar{h_0}^2}{6\beta^2}a$, and let us define

$$\mathcal{H} = \frac{1}{2}\int_\Omega h_0^2 + \varepsilon^2\|\mathbf{grad}h_0\|^2. \tag{9}$$

Note that a closely related Hamiltonian functional, involving both the variable and its gradient serves as a basis for the derivation and simulation of dynamics in materials with a nonlocal constitutive relation [1].

Let us then compute $\frac{\mathrm{d}}{\mathrm{d}t}\mathcal{H}$, the power balance

$$\begin{aligned}
\frac{\mathrm{d}}{\mathrm{d}t}\mathcal{H} &= \int_\Omega h_0\frac{\partial h_0}{\partial t} + \varepsilon^2\mathbf{grad}h_0\cdot\mathbf{grad}\frac{\partial h_0}{\partial t}\\
&= \int_\Omega h_0(1-\varepsilon^2\Delta)\frac{\partial h_0}{\partial t} + \varepsilon^2\int_{\partial\Omega} h_0\left(\mathbf{grad}\frac{\partial h_0}{\partial t}\right)\cdot\mathbf{n}\\
&= \int_\Omega h_0\left(a\Delta h_0 - b\Delta^2 h_0\right) + \varepsilon^2\int_{\partial\Omega} h_0\left(\mathbf{grad}\frac{\partial h_0}{\partial t}\right)\cdot\mathbf{n},\\
&= -\int_\Omega a\mathbf{grad}h_0\cdot\mathbf{grad}h_0 - \int_\Omega b\Delta h_0\Delta h_0\\
&\quad + \int_{\partial\Omega} ah_0\mathbf{grad}h_0\cdot\boldsymbol{n} - \int_{\partial\Omega} bh_0\ \mathbf{grad}(\Delta h_0)\cdot\boldsymbol{n}\\
&\quad + \int_{\partial\Omega} b\Delta h_0\mathbf{grad}(h_0)\cdot\boldsymbol{n} + \varepsilon^2\int_{\partial\Omega} h_0\left(\mathbf{grad}\frac{\partial h_0}{\partial t}\right)\cdot\mathbf{n},\\
&\le \int_{\partial\Omega} ah_0\mathbf{grad}h_0\cdot\boldsymbol{n} - \int_{\partial\Omega} bh_0\ \mathbf{grad}(\Delta h_0)\cdot\boldsymbol{n}\\
&\quad + \int_{\partial\Omega} b(\mathbf{grad}(h_0)\cdot\boldsymbol{n})\Delta h_0 + \varepsilon^2\int_{\partial\Omega} h_0\left(\mathbf{grad}\frac{\partial h_0}{\partial t}\right)\cdot\mathbf{n}.
\end{aligned} \tag{10}$$

[1] see e. g. the documentation of Code ASTER, §5.7, Keyword factor NON_LOCAL `https://code-aster.org/V2/doc/default/en/man_u/u4/u4.43.01.pdf`

And the system can be restated as follows

$$\begin{pmatrix}(1-\varepsilon^2\Delta)\frac{\partial h_0}{\partial t}\\ \mathbf{grad}h_0\\ \Delta h_0\end{pmatrix} = \begin{pmatrix}0 & \mathrm{div} & -\Delta\\ \mathbf{grad} & 0 & 0\\ \Delta & 0 & 0\end{pmatrix}\begin{pmatrix}h_0\\ a\,\mathbf{grad}h_0\\ b\,\Delta h_0\end{pmatrix}. \tag{11}$$

As a consequence, natural boundary controls appear in the boundary terms of the power balance (10), such as the flux

$$(a\mathbf{grad}(h_0) - b\mathbf{grad}(\Delta h_0))\cdot\boldsymbol{n}, \tag{12}$$

and the pressure normal derivative, and its time derivative

$$\mathbf{grad}(h_0)\cdot\boldsymbol{n}, \qquad \mathbf{grad}\left(\frac{\partial h_0}{\partial t}\right)\cdot\boldsymbol{n}. \tag{13}$$

Remark 3 In (11), the Laplacian operator in front of the time derivative $\partial_t h_0$ is very reminiscent of a similar situation for the numerical treatment of the incompressible Navier-Stokes equations, studied e.g. in Haine and Matignon (2021). Indeed in this latter case, minus the Laplacian operator was included in the constitutive equations relating the vorticity ω and the stream function ψ. The appearance of the time derivative of the boundary control is related to the index 2 of the underlying Differential Algebraic Equation (DAE), see e.g. Mehrmann and Unger (2022) and references therein.

3.2 The Partitioned Finite Element Method for pHDAE

Let us define $\begin{pmatrix}f_{\mathbf{grad}} = \mathbf{grad}(h_0)\\ e_{\mathbf{grad}} = af_{\mathbf{grad}}\end{pmatrix}$ and $\begin{pmatrix}f_\Delta = \Delta h_0\\ e_\Delta = bf_\Delta\end{pmatrix}$.

Variational formulation Let us choose two scalar test functions $\lambda_1, \lambda_2 \in C^\infty(\Omega,\mathbb{R})$ and a vector-valued test function $\boldsymbol{\phi} \in C^\infty(\Omega,\mathbb{R}^2)$.

Let us write the variational formulation of the system

$$\begin{cases}\int_\Omega \lambda_1(1-\varepsilon^2\Delta)\partial_t h_0 = \int_\Omega \lambda_1(\ \mathrm{div}(e_{\mathbf{grad}}) - \Delta(e_\Delta)),\\ \int_\Omega \boldsymbol{\phi}\cdot f_{\mathbf{grad}} = \int_\Omega \boldsymbol{\phi}\cdot\mathbf{grad}(h_0),\\ \int_\Omega \lambda_2 f_\Delta = \int_\Omega \lambda_2\Delta h_0,\end{cases} \tag{14}$$

together with the constitutive relations

$$\begin{cases}\int_\Omega \boldsymbol{\phi}\cdot e_{\mathbf{grad}} = \int_\Omega \boldsymbol{\phi}\cdot af_{\mathbf{grad}},\\ \int_\Omega \boldsymbol{\phi}\cdot e_\Delta = \int_\Omega \boldsymbol{\phi}\cdot bf_\Delta.\end{cases} \tag{15}$$

Choice of causality In order to control the system, we propose to prescribe the boundary values of the flux (12) with a control u_f and the normal derivative of the pressure and its time derivative (13) with a pair of controls u_p and $\partial_t u_p$.

By integrating by parts the terms on the left and right-hand side of the first line of (14) and the right-hand side of the third line of (14), we obtain

$$\int_\Omega \lambda_2 f_\Delta = -\int_\Omega \mathbf{grad}\lambda_2\cdot\mathbf{grad}h_0 + \int_{\partial\Omega}\lambda_2\underbrace{\mathbf{grad}h_0\cdot\boldsymbol{n}}_{=u_p},$$

and

$$\int_\Omega \lambda_1 \partial_t h_0 + \varepsilon^2 \,\mathbf{grad}\lambda_1 \cdot \mathbf{grad}\partial_t h_0 = \int_{\partial\Omega} \lambda_1 \,\varepsilon^2 \underbrace{\mathbf{grad}\partial_t h_0 \cdot \boldsymbol{n}}_{=\partial_t u_p} - \int_\Omega \mathbf{grad}(\lambda_1)\cdot(e_{\mathbf{grad}} - \mathbf{grad}(e_\Delta)) + \int_{\partial\Omega} \lambda_1 \underbrace{(e_{\mathbf{grad}} - \mathbf{grad}(e_\Delta))\cdot \boldsymbol{n}}_{=u_f},$$

respectively. The two boundary controls appear now in the variational formulation, and we are in position to apply a finite element method.

Finite element families Let us choose four finite element families: $(\lambda_{1,i})_{i\in[\![1,n_1]\!]}$, $(\lambda_{2,i})_{i\in[\![1,n_2]\!]} \in H^1(\Omega)$, $(\boldsymbol{\phi}_i)_{i\in[\![1,n_3]\!]} \in H^1(\Omega,\mathbb{R}^2)$, $(\psi_i^f)_{i\in[\![1,m_f]\!]}, (\psi_i^p)_{i\in[\![1,m_p]\!]} \in H^{\frac{1}{2}}(\partial\Omega)$, of size n_1, n_2, n_3, m_f, and m_p respectively.

In the sequel, we denote $\underline{\circ}$ the column vector of the coefficients of $\circ^d$, the discretization of the quantity $\circ$ in its finite element basis. As an exemple, $\underline{u}_f := (\underline{u}_f^i)_{i\in[\![1,m_f]\!]}$, where $u_f^d := \sum_{i=1}^{m_f} \psi_i^f \underline{u}_f^i$ denotes the discretization of u_f in its basis $(\psi_i^f)_i$.

Let us note

$$\begin{cases} \mathbf{M}_k := \left(\int_\Omega \lambda_{k,i}\lambda_{k,j}\right)_{i,j\in[\![1,n_k]\!]}, k\in\{1,2\}, \\ \mathbf{M}_{\boldsymbol{\phi}} := \left(\int_\Omega \boldsymbol{\phi}_i\cdot\boldsymbol{\phi}_j\right)_{i,j\in[\![1,n_3]\!]}, \end{cases}$$

the mass matrices.

Let us note

$$\mathbf{K} := \left(\int_\Omega \mathbf{grad}(\lambda_{1,i})\cdot\mathbf{grad}(\lambda_{1,j})\right)_{i,j\in[\![1,n_1]\!]}.$$

The full mass matrix is then

$$\mathbf{M}_\varepsilon := \begin{pmatrix} (\mathbf{M}_1+\varepsilon^2\mathbf{K}) & 0 & 0 \\ 0 & \mathbf{M}_{\boldsymbol{\phi}} & 0 \\ 0 & 0 & \mathbf{M}_2 \end{pmatrix}.$$

Note furthermore

$$\mathbf{D}_{\mathbf{grad}} := \left(-\int_\Omega \mathbf{grad}(\lambda_{1,i})\cdot\boldsymbol{\phi}_j\right)_{i\in[\![1,n_1]\!],j\in[\![1,n_3]\!]},$$

the first structure matrix, and

$$\mathbf{D}_\Delta := \left(\int_\Omega \mathbf{grad}(\lambda_{1,i})\cdot\mathbf{grad}(\lambda_{2,j})\right)_{i\in[\![1,n_1]\!],j\in[\![1,n_2]\!]},$$

the second structure matrix.

The full structure matrix is then

$$\mathbf{J} := \begin{pmatrix} 0 & \mathbf{D}_{\mathbf{grad}} & \mathbf{D}_\Delta \\ -\mathbf{D}_{\mathbf{grad}}^T & 0 & 0 \\ -\mathbf{D}_\Delta^T & 0 & 0 \end{pmatrix}.$$

Now, denoting

$$\mathbf{B}_f := \left(\int_{\partial\Omega} \lambda_{1,i}\psi_j^f\right)_{i\in[\![1,n]\!],j\in[\![1,m_f]\!]},$$

$$\mathbf{B}_{p,k} := \left(\int_{\partial\Omega} \lambda_{k,i}\psi_j^p\right)_{i\in[\![1,n]\!],j\in[\![1,m_p]\!]}, \forall k\in\{1,2\}$$

the control matrices, and $\mathbf{C}_a := a\mathbf{M}_{\boldsymbol{\phi}}$ and $\mathbf{C}_b := b\mathbf{M}_2$ the two constitutive matrices, the spatial discretization of (14)–(15) reads

$$\begin{cases} \mathbf{M}_\varepsilon \begin{pmatrix} \frac{d}{dt}\underline{h_0} \\ \underline{f_{\mathbf{grad}}} \\ \underline{f_\Delta} \end{pmatrix} = \mathbf{J}\begin{pmatrix} \underline{h_0} \\ \underline{e_{\mathbf{grad}}} \\ \underline{e_\Delta} \end{pmatrix} + \begin{pmatrix} \mathbf{B}_f & 0 & \varepsilon^2\mathbf{B}_{p,1} \\ 0 & 0 & 0 \\ 0 & \mathbf{B}_{p,2} & 0 \end{pmatrix}\begin{pmatrix} \underline{u}_f \\ \underline{u}_p \\ \frac{d}{dt}\underline{u}_p \end{pmatrix}, \\ \begin{pmatrix} \mathbf{M}_{\boldsymbol{\phi}} & 0 \\ 0 & \mathbf{M}_2 \end{pmatrix}\begin{pmatrix} \underline{e_{\mathbf{grad}}} \\ \underline{e_\Delta} \end{pmatrix} = \begin{pmatrix} \mathbf{C}_a & 0 \\ 0 & \mathbf{C}_b \end{pmatrix}\begin{pmatrix} \underline{f_{\mathbf{grad}}} \\ \underline{f_\Delta} \end{pmatrix}. \end{cases} \quad (16)$$

3.3 Discrete power balance

Let us define the discrete Hamiltonian as the continuous one, defined in (9), evaluated on the approximated variable h_0^d. Namely

$$\mathcal{H}^{\mathrm{d}} := \frac{1}{2}\int_\Omega (h_0^d)^2 + \varepsilon^2\|\mathbf{grad}h_0^d\|^2., \\ = \frac{1}{2}(\underline{h_0}^\top\mathbf{M}_1\underline{h_0} + \varepsilon^2\underline{h_0}^\top\mathbf{K}\underline{h_0}).$$

Then, we can compute the discrete power balance

$$\begin{aligned} \frac{d}{dt}\mathcal{H}^{\mathrm{d}} &= \frac{d}{dt}(\frac{1}{2}(\underline{h_0}^\top\mathbf{M}_1\underline{h_0} + \underline{h_0}^\top\varepsilon^2\mathbf{K}\underline{h_0}), \\ &= \underline{h}_0^\top(\mathbf{M}_1+\varepsilon^2\mathbf{K})\frac{d}{dt}\underline{h}_0, \\ &= \underline{h}_0^\top(\mathbf{D}_{\mathbf{grad}}\underline{e}_{\mathbf{grad}} + \mathbf{D}_\Delta\underline{e}_\Delta + \mathbf{B}_f\underline{u}_f + \varepsilon^2\mathbf{B}_{p,1}\frac{d}{dt}\underline{u}_p), \\ &= -\underline{f}_{\mathbf{grad}}^\top\mathbf{M}_{\boldsymbol{\phi}}\underline{e}_{\mathbf{grad}} - \underline{f}_\Delta^\top\mathbf{M}_2\underline{e}_\Delta + \underline{u}_p^\top\mathbf{B}_{p,2}^\top\underline{e}_\Delta \\ &\quad + \underline{h}_0^\top\mathbf{B}_f\underline{u}_f + \varepsilon^2\underline{h}_0^\top\mathbf{B}_{p,1}\frac{d}{dt}\underline{u}_p, \\ &= -a\,\underline{f}_{\mathbf{grad}}^\top\mathbf{M}_{\boldsymbol{\phi}}\underline{f}_{\mathbf{grad}} - b\,\underline{f}_\Delta^\top\mathbf{M}_2\underline{f}_\Delta + \underline{e}_\Delta^\top\mathbf{B}_{p,2}\underline{u}_p \\ &\quad + \underline{h}_0^\top\mathbf{B}_f\underline{u}_f + \varepsilon^2\underline{h}_0^\top\mathbf{B}_{p,1}\frac{d}{dt}\underline{u}_p, \\ &\leq \begin{pmatrix} \underline{y}_f \\ \underline{y}_p \\ \underline{y}_{\mathrm{d}_tp} \end{pmatrix}^\top \begin{pmatrix} \mathbf{M}_f^\partial & 0 & 0 \\ 0 & \mathbf{M}_p^\partial & 0 \\ 0 & 0 & \mathbf{M}_p^\partial \end{pmatrix}\begin{pmatrix} \underline{u}_f \\ \underline{u}_p \\ \frac{d}{dt}\underline{u}_p \end{pmatrix}, \end{aligned} \quad (17)$$

where the symmetric boundary mass matrices are given by

$$\mathbf{M}_k^\partial := \left(\int_{\partial\Omega}\psi_i^k\psi_j^k\right)_{i,j\in[\![1,m_k]\!]}, k\in\{f,p\},$$

and the collocated outputs are defined by

$$\begin{pmatrix} \mathbf{M}_f^\partial & 0 & 0 \\ 0 & \mathbf{M}_p^\partial & 0 \\ 0 & 0 & \mathbf{M}_p^\partial \end{pmatrix}\begin{pmatrix} \underline{y}_f \\ \underline{y}_p \\ \underline{y}_{\mathrm{d}_tp} \end{pmatrix} = \begin{pmatrix} \mathbf{B}_f^\top & 0 & 0 \\ 0 & 0 & \mathbf{B}_{p,2}^\top \\ \varepsilon^2\mathbf{B}_{p,1}^\top & 0 & 0 \end{pmatrix}\begin{pmatrix} \underline{h}_0 \\ \underline{e}_{\mathbf{grad}} \\ \underline{e}_\Delta \end{pmatrix}.$$

Then (17) mimics (10).

3.4 Numerical Simulations

For these tests, performed using SCRIMP environment [2], the Finite Elements (FE) are chosen as follows: the hydraulic head h_0, f_Δ and e_Δ are approximated by Continuous Galerkin FE of order 1 (CG1), *i.e.* $\lambda_1 = \lambda_2 \simeq$

[2] https://g-haine.github.io/scrimp/

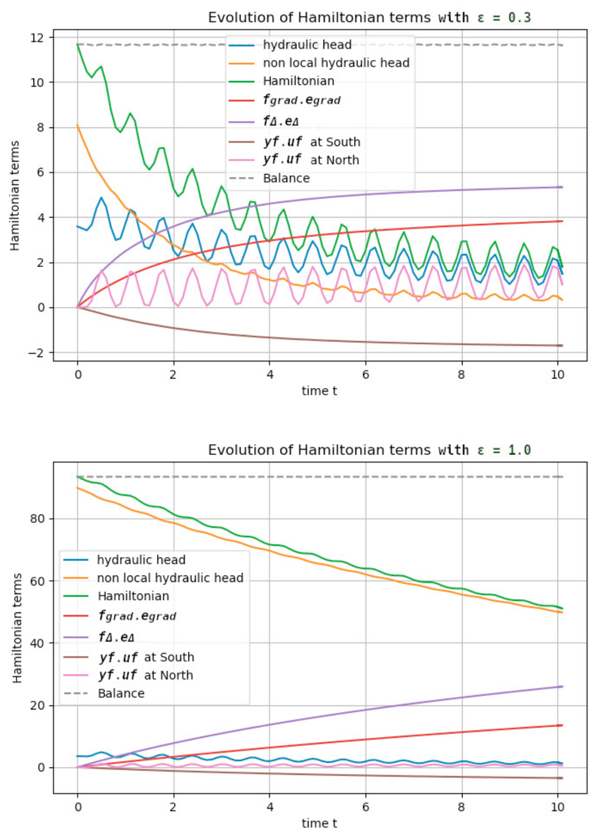

Figure 1. The 2D Dzektser model, with the same damping parameters $a = 0.01, b = 0.0001$, and two non-local parameters $\varepsilon = 0.3$ (top) and $\varepsilon = 1$ (bottom).

CG1, $f_{\mathbf{grad}}$ and $e_{\mathbf{grad}}$ are approximated by Discontinuous Galerkin FE of order 1 (DG1), *i.e.* $\Phi \simeq$ DG1, while the boundary ports are approximated by Continous Galerkin FE of order 1, *i.e.* $\psi^p = \psi^f \simeq$ CG1. The time integration of the resulting differential algebraic equation is performed using the Crank-Nicolson time-stepper available in PETSc TS.

Let us consider $\Omega = [0,1]^2$ with boundaries North, West, South and East. The initial datum is $h_0(x, y, t = 0) = (1.+\sin(8x)) * (1 + \sin(10y)) + 1 + \cos(7y) * \sin(6x))$. At the South boundary, the control is taken in order to observe a monotonic power flow: $u_f^{\text{South}}(x) = -0.1 * h_0(x, 0, t)$ (brown curves on Figure 1) and at the North, u_f^{North} is taken as an oscillating signal in order to induce a sufficiently large gradient $\mathbf{grad} h_0$ in the system. This will help to appreciate how the non-local parameter ε acts *via* the dissipative ports. All the other controls are taken equal to zero.

Figure 1 compares the evolution of the energies of the system for two different values of ε: on the first plot, the non-local parameter is small, $\varepsilon = 0.3$, while on the second plot, it is taken as $\varepsilon = 1$. Care must be taken that ε appears explicitly in the definition of the Hamiltonian: this dependence explains the change of scale between the two plots of Figure 1 while the other parameters remain identical.

A focus on the term $\frac{1}{2} \int_\Omega \varepsilon^2 \|\mathbf{grad} h_0\|^2$, the so-called *non-local hydraulic head* represented by the orange curves, enlights the role of the ε parameter: when ε is small, oscillations induced by the control at the North boundary propagate easily through the domain: thus, the hydraulic head h_0 presents variations which imply large enough values of its gradient allowing for the observation of quite a strong dissipation through the dissipative ports $f_{\mathbf{grad}} = \mathbf{grad} h_0$ and $f_\Delta = \Delta h_0$. On the contrary, increasing ε makes the system move as a whole since the control has an immediate effect on a larger band of the domain: this, in turn, implies smaller variations of h_0, hence of its gradient, and the dissipation becomes even slower.

Finally, one can appreciate the structure-preserving property of the method, looking at the *Balance* in dashed lines on Figure 1, which represent the power balance in its integral form; in other words, the value of

$$\texttt{Balance} = \mathcal{H}^d(t) + \int_0^t \left(\underline{f}_{\mathbf{grad}}^\top \mathbf{M}_\Phi \underline{e}_{\mathbf{grad}} + \underline{f}_\Delta^\top \mathbf{M}_2 \underline{e}_\Delta \right) - \int_0^t \left(\underline{y}_f^\top \mathbf{M}_f^\partial \underline{u}_f + \underline{y}_p^\top \mathbf{M}_p^\partial \underline{u}_p + \underline{y}_{\mathrm{d}_t p}^\top \mathbf{M}_f^\partial \frac{d}{dt} \underline{u}_p \right)$$

remains constant in time.

4. CONCLUSION AND OUTLOOK

So far, a structure-preserving discretization method has been extended to two types of implicit pHs, one in 1D with a singular matrix, and another one in 2D with an unbounded differential operator: indeed, at the discrete level PFEM is able to mimic the energy balance of the implicit system with collocated boundary control and observation, both in the lossless and lossy cases. Simulation results have been successfully performed for the 2D seepage model, showing the expected Hamiltonian behaviour.

In the near future, several tracks can be investigated: on the one hand, it is possible to apply PFEM further in trying to take advantage of another factorization of the nano-rod model as recently proposed in Heidari and Zwart (2022), or in extending the nano-rod model to the 2D case; also addressing the special damping class of AR-MA type as introduced in Matignon and Hélie (2013) will be possible, since this class directly falls in the case of implicit constitutive relations. On the other hand, working in depth on the port-Hamiltonian formulations of fluid filtration models is also another promising line of research, trying to tackle e.g. generalized Boussinesq equation following Maschke and van der Schaft (2013); Perevozhikova and Manakova (2021), and then applying PFEM to it.

5. SPECIAL THANKS

The authors would like to thank Vsevolod Peysakovich, from ISAE-DCAS, for the translation of Dzektser (1972).

REFERENCES

Altmann, R. and Schulze, P. (2017). A port-Hamiltonian formulation of the Navier–Stokes equations for reactive flows. *Systems Control Letters*, 100, 51–55. doi: https://doi.org/10.1016/j.sysconle.2016.12.005.

Beattie, C., Mehrmann, V., Xu, H., and Zwart, H. (2018). Linear port-Hamiltonian descriptor systems. *Mathematics of Control, Signals, and Systems*, 30(4), 17.

Bendimerad-Hohl, A., Haine, G., Matignon, D., and Maschke, B. (2022). Structure-preserving discretization of a coupled Allen-Cahn and heat equation system. In *IFAC-PapersOnLine*, volume 55, 99–104. doi: 10.1016/j.ifacol.2022.08.037.

Brugnoli, A., Haine, G., Serhani, A., and Vasseur, X. (2021). Numerical approximation of port-Hamiltonian systems for hyperbolic or parabolic PDEs with boundary control. *Journal of Applied Mathematics and Physics*, 9(6), 1278–1321. doi:10.4236/jamp.2021.96088.

Brugnoli, A., Alazard, D., Pommier-Budinger, V., and Matignon, D. (2019). Port-Hamiltonian formulation and symplectic discretization of plate models Part II: Kirchhoff model for thin plates. *Applied Mathematical Modelling*, 75, 961–981. doi:10.1016/j.apm.2019.04.036.

Cardoso-Ribeiro, F.L., Brugnoli, A., Matignon, D., and Lefèvre, L. (2019). Port-Hamiltonian modeling, discretization and feedback control of a circular water tank. In *58th IEEE Conf. on Decision and Control (CDC)*, 6881–6886. Nice, France. Invited session.

Cardoso-Ribeiro, F.L., Matignon, D., and Lefèvre, L. (2021). A partitioned finite-element method for power-preserving discretization of open systems of conservation laws. *IMA J. Mathematical Control and Information*, 38(2), 493–533. doi:10.1093/imamci/dnaa038.

Duindam, V., Macchelli, A., Stramigioli, S., and Bruyninckx, H. (2009). *Modeling and control of complex physical systems: the port-Hamiltonian approach*. Springer Science & Business Media.

Dzektser, E.S. (1972). Generalization of the equation of motion of ground waters with free surface. *Dokl. Akad. Nauk SSSR*, 202(5), 1031–1033.

Eringen, A.C. (1983). On differential equations of nonlocal elasticity and solutions of screw dislocation and surface waves. *J. Appl. Phys.*, 54(9), 4703–4710.

Fedorov, V.E. and Shklyar, B. (2012). Exact null controllability of degenerate evolution equations with scalar control. *Sbornik : Mathematics*, 203(12), 1817–1836.

Ge, Z., Ge, X., and Zhang, J. (2020). Approximate controllability and approximate observability of singular distributed parameter systems. *IEEE Trans. Autom. Control*, 65(5), 2294–2299.

Haine, G. and Matignon, D. (2021). Incompressible Navier-Stokes Equation as port-Hamiltonian systems: velocity formulation versus vorticity formulation. In *IFAC-PapersOnLine*, volume 54, 161–166. doi: doi.org/10.1016/j.ifacol.2021.11.072.

Haine, G., Matignon, D., and Serhani, A. (2023). Numerical analysis of a structure-preserving space-discretization for an anisotropic and heterogeneous boundary controlled N-dimensional wave equation as a port-Hamiltonian system. *Int. J. Numer. Anal. Mod.*, 20(1), 92–133. doi:10.4208/ijnam2023-1005.

Heidari, H. and Zwart, H. (2019). Port-Hamiltonian modelling of nonlocal longitudinal vibrations in a viscoelastic nanorod. *Mathematical and Computer Modelling of Dynamical Systems*, 25(5), 447–462.

Heidari, H. and Zwart, H. (2022). Nonlocal longitudinal vibration in a nanorod, a system theoretic analysis. *Math. Model. Nat. Phenom.*, 17, 24.

Jacob, B. and Morris, K. (2022). On solvability of dissipative partial differential-algebraic equations. *IEEE Control. Syst. Lett.*, 6, 3188–3193.

Jacob, B. and Zwart, H.J. (2012). *Linear port-Hamiltonian systems on infinite-dimensional spaces*, volume 223. Springer Science & Business Media.

Kotyczka, P., Maschke, B., and Lefèvre, L. (2018). Weak form of Stokes–Dirac structures and geometric discretization of port-Hamiltonian systems. *Journal of Computational Physics*, 361, 442–476.

Kurula, M. and Zwart, H. (2015). Linear wave systems on n-D spatial domains. *International Journal of Control*, 88(5), 1063–1077.

Maschke, B. and van der Schaft, A. (2013). On alternative Poisson brackets for fluid dynamical systems and their extension to Stokes-Dirac structures. In *IFAC Proceedings Volumes*, volume 46, 109–114.

Matignon, D. and Hélie, T. (2013). A class of damping models preserving eigenspaces for linear conservative port-Hamiltonian systems. *European Journal of Control*, 19(6), 486–494. doi:10.1016/j.ejcon.2013.10.003.

Mehrmann, V. and Morandin, R. (2019). Structure-preserving discretization for port-Hamiltonian descriptor systems. In *58th IEEE Conf. on Decision and Control (CDC)*, 6863–6868. Nice, France. Invited session.

Mehrmann, V. and Unger, B. (2022). Control of port-Hamiltonian differential-algebraic systems and applications. *arXiv:2201.06590*.

Mehrmann, V. and van der Schaft, A. (2023). Differential–algebraic systems with dissipative Hamiltonian structure. *Mathematics of Control, Signals, and Systems*. doi:10.1007/s00498-023-00349-2.

Perevozhikova, K.V. and Manakova, N.A. (2021). Numerical simulation of start control and final observation in fluid filtration model. *J. Comp. Eng. Math.*, (1), 29–45.

Rashad, R., Califano, F., van der Schaft, A., and Stramigioli, S. (2020). Twenty years of distributed port-Hamiltonian systems: a literature review. *IMA J. Mathematical Control and Information*, 37(4), 1400–1422.

van der Schaft, A. and Maschke, B. (2002). Hamiltonian formulation of distributed-parameter systems with boundary energy flow. *Journal of Geometry and Physics*, 42(1-2), 166–194.

van der Schaft, A. and Maschke, B. (2020). Dirac and Lagrange algebraic constraints in nonlinear Port-Hamiltonian systems. *Vietnam Journal of Mathematics*, 48, 929–939. doi:10.1007/s10013-020-00419-x.

van der Schaft, A., Jeltsema, D., et al. (2014). Port-Hamiltonian systems theory: An introductory overview. *Foundations and Trends® in Systems and Control*, 1(2-3), 173–378.

van der Schaft, A. and Maschke, B. (2018). Generalized port-Hamiltonian DAE systems. *Systems and Control Letters*, 121, 31–37. doi:10.1016/j.sysconle.2018.09.008.

Vu, N.M.T., Lefevre, L., and Maschke, B. (2016). A structured control model for the thermo-magneto-hydrodynamics of plasmas in tokamaks. *Mathematical and comput. modelling of dyn systems*, 22(3), 181–206.

Yaghi, M., Couenne, F., Galfré, A., Lefèvre, L., and Maschke, B. (2022). Port-Hamiltonian formulation of the solidification process for a pure substance: A phase field approach. In *IFAC-PapersOnLine*, volume 55, 93–98. doi:10.1016/j.ifacol.2022.08.036.